

Sum-frequency generation of 589 nm light with near-unit efficiency

Emmanuel Mimoun¹, Luigi De Sarlo¹, Jean-Jacques Zondy², Jean Dalibard¹, and Fabrice Gerbier¹

¹ Laboratoire Kastler Brossel, ENS, Université Pierre et Marie-Curie-Paris 6, CNRS, 24 rue Lhomond, 75005 Paris, France.

² Institut National de Métrologie (LNE-INM-Cnam), 61 rue du Landy, 93210 La Plaine Saint Denis, France.

Compiled November 29, 2018

We report on a laser source at 589 nm based on sum-frequency generation of two infrared laser at 1064 nm and 1319 nm. Output power as high as 790 mW are achieved starting from 370 mW at 1319 nm and 770 mW at 1064 nm, corresponding to converting roughly 90% of the 1319 nm photons entering the cavity. © 2018 Optical Society of America

OCIS codes: 140.3580, 190.4360

Although the range of optical wavelengths that can be reached with solid-state lasers keeps broadening, building a cost-effective solution to produce a powerful single-frequency laser source in the yellow-orange (550 – 600 nm) spectral range remains an open challenge. Non-solid options such as dye lasers or copper vapor lasers have been used for a long time, but they are expensive and difficult to maintain and operate. An alternative approach uses non-linear processes to generate visible light from solid-state infrared lasers [1–9]. Second harmonic generation from a Raman fiber laser [1–3], and sum frequency generation (SFG) from two lasers around 938 nm and 1535 nm [4], or around $\lambda_1 = 1064$ nm and $\lambda_2 = 1319$ nm, have been demonstrated. The latter solution is particularly appealing, both wavelengths being accessible using YAG lasers. Such infrared sources have been used in both single-pass [5] (generating little power) and cavity-enhanced configurations [6–9]. However, to our knowledge, no such system has combined a narrow linewidth ($\lesssim 1$ MHz), and an output power in the watt-level range using commercial infrared sources.

In this Letter, we present a setup producing up to $P_3 \approx 790$ mW at $\lambda_3 = 589$ nm using $P_1 \approx 770$ mW at 1064 nm and $P_2 \approx 370$ mW at 1319 nm coupled into a doubly resonant cavity¹. This corresponds to converting roughly 90% of the photons of the weakest (1319nm) source. We use a periodically poled KTiOPO₄ (ppKTP) crystal, which has a relatively high non-linear coefficient, tolerates large input powers, and has negligible absorption in the visible range. The high depletion of the 1319 nm pump source at such efficiencies significantly distorts the cavity fringe pattern, requiring an original fringe reshaping method to efficiently and robustly lock the lasers to the cavity. The resulting 589 nm laser source allows us to laser cool sodium atoms, the primary motivation behind this work. To our knowledge, this had only been achieved previously using dye lasers (see *e.g.* [10, 11]).

Our system is described schematically in Fig. 1a. Lasers 1 and 2 are coupled into a bow-tie cavity, which is resonant for both of them but transparent for the output laser at λ_3 . Let

¹We use commercial sources (manufactured by Innolight GmbH, Germany) delivering 500 mW at 1319 nm and 1 W at 1064 nm. Losses through the optical path and a 85% coupling efficiency into the cavity result in a useful power as quoted in text.

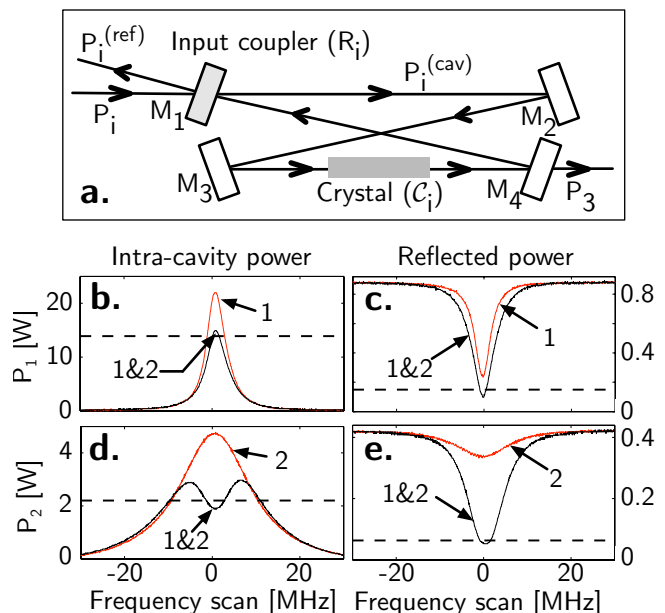


Figure 1: **a.** Setup for SFG in a doubly resonant cavity. For the pump lasers i ($i = 1, 2$), we note $P_i^{(cav)}$ the intra-cavity power, P_i the incident power and $P_i^{(ref)}$ the reflected power; **b-d.** Intra-cavity powers for lasers 1 (**b**) and 2 (**d**) ($\lambda_1 = 1064$ nm, $\lambda_2 = 1319$ nm), plotted against the cavity resonance frequency tuned with a piezoelectric transducer; **c-e.** Powers reflected out of the cavity for lasers 1 (**c**) and 2 (**e**). The dashed lines show the predictions from the model described in the text, which includes both conversion and passive losses.

us first consider an ideal situation with no passive losses in the cavity, and where the input coupler M_1 has a reflectivity $R_i < 1$ for laser i ($i = 1, 2$). We assume that only a small fraction of the intra-cavity powers is consumed in the SFG process. In this weakly-depleted pumps approximation, the output power P_3 at wavelength λ_3 is given by [12–14]:

$$P_3 = \alpha P_1^{(cav)} P_2^{(cav)}. \quad (1)$$

On resonance, the intra-cavity power $P_i^{(cav)}$ is linked to the

incident power P_i by [15]

$$\frac{P_i^{(\text{cav})}}{P_i} = \frac{1 - R_i}{(1 - \sqrt{R_i C_i})^2}, \quad (2)$$

where the coefficient C_i , the ratio between the photon flux before and after the crystal, accounts for the depletion of laser i due to SFG. Neglecting absorption in the crystal, energy conservation in the conversion process implies $C_i = 1 - \lambda_3 P_3 / \lambda_i P_i^{(\text{cav})}$. As long as $C_i \simeq 1$, the weakly depleted pumps approximation is valid. Ultimately, the efficiency of SFG is limited by the weakest pump 2. The maximal output flux at λ_3 equals the input flux at λ_2 , corresponding to $P_3^{(\text{max})} = (\lambda_2 / \lambda_3) P_2$. In this optimal situation where complete conversion occurs, we find $C_2^{\text{opt}} = R_2$ and a cavity enhancement factor $P_2^{(\text{cav})} / P_2 = (1 - R_2)^{-1}$: the input coupler of the cavity lets in exactly what the crystal consumes (impedance matching condition [16]). This situation is fully compatible with the weakly-depleted pumps approximation. Indeed, because of the cavity power enhancement, the small fraction of the intra-cavity power consumed in the crystal can approach the incident flux.

Interestingly, the power reflected at mirror M_1

$$\frac{P_2^{(\text{ref})}}{P_2} = \frac{(\sqrt{C_2} - \sqrt{R_2})^2}{(1 - \sqrt{R_2 C_2})^2}. \quad (3)$$

vanishes under these optimum conditions: all the incoming photons are converted in the crystal and no photon at λ_2 comes out of the cavity. This can be interpreted as a destructive interference on M_1 between the reflected field and the transmitted one. In the following, we take the ratio $\eta = \lambda_3 P_3 / \lambda_2 P_2$ between the outgoing flux at λ_3 and the limiting incoming flux at λ_2 as a figure of merit for the conversion efficiency.

The results above, though only valid in the lossless case, can be used to interpret qualitatively our experimental findings. In Fig. 1 we show the transmitted (**b,d**) and reflected (**c,e**) power while scanning the cavity length around the position where both lasers are simultaneously resonant. When only one laser is present (either 1 or 2) we observe the expected Lorentzian profile. However when both lasers are present a pronounced dip appears in the resonance profile for laser 2, corresponding to efficient conversion into 589 nm photons. A dramatic decrease of the reflected power is simultaneously observed, corresponding to the destructive interference previously mentioned. Experimentally, this leads to serious stability problems. The key to efficient operation is to ensure that both IR lasers are simultaneously resonant into the cavity. This is usually enforced by using two servo-loops to maximize the intra-cavity power, monitoring for each laser the power leaking from the cavity. Although this scheme is standard for a SFG setup, it leads to serious stability problems in the regime of large conversion described above. Indeed, when the cavity is locked to laser 2 in the presence of laser 1, non-linear conversion significantly reduces $P_2^{(\text{cav})}$ (see Fig. 1d). The cavity servo cannot distinguish this power

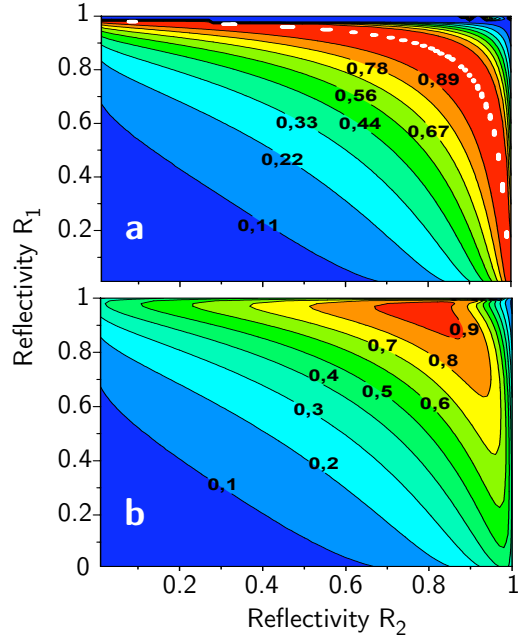


Figure 2: (color online) Contour map of the efficiency η of the conversion process as a function of the reflectivities R_1 and R_2 of the input coupler M_1 for laser 1 and 2 ($\lambda_1 = 1064$ nm and $\lambda_2 = 1319$ nm). **a.** Lossless case. The dashed line corresponds to total conversion ($\eta = 1$). **b.** Passive losses are taken into account using the values found. While $\eta = 1$ cannot be obtained anymore experimentally, efficiencies higher than 90% can still be reached.

reduction from that caused by an external perturbation, and actually works against keeping both lasers on resonance simultaneously. One is led to decrease the servo gain to acquire lock at all, thus diminishing the overall stability.

To circumvent this problem, we have designed and implemented the following locking scheme. Instead of the bare cavity transmission at λ_2 , we take as the error signal for the cavity lock a linear combination of this cavity transmission and of the output at λ_3 . The combination is done electronically, with weights chosen empirically to reproduce the smooth lineshape of the resonance of a single laser in the cavity. This fringe reshaping method works well even at the highest efficiencies (see below). Finally, choosing the 589 nm output as the error signal for the second servo-loop ensures that the system locks to the maximal converted power².

As discussed above, for each value of the input coupler reflectivity R_2 , all incoming photons are converted when $P_2^{(\text{cav})} = P_2 / (1 - R_2)$. Eq. (1) then fixes the corresponding value for $P_1^{(\text{cav})} = (1 - R_2) \lambda_2 / \alpha \lambda_3$, which is achieved for a reflectivity R_1 following from Eq. (2). Therefore, total conversion can be obtained in the lossless case for any value of R_2 (see dashed line in Fig. 2a).

In a more realistic model, which includes passive losses,

²The locking system is protected by French patent 0803153, international patent pending. The detailed technical realization will be described in a future publication [17].

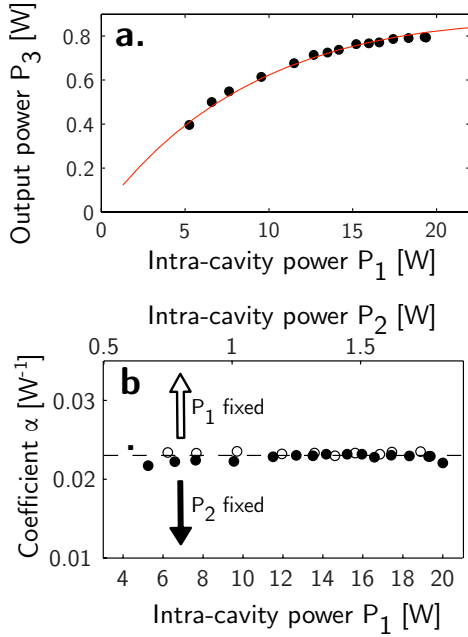


Figure 3: **a.** Output power at 589 nm plotted against intra-cavity power at 1064 nm (varied by changing the incoming power into the cavity). The solid line is the result of the numerical calculations as described in text. **b.** Conversion coefficient α (see Eq. (1)), varying the incoming power of one pump laser while leaving the other fixed. The conversion coefficient is constant and equal to that measured in the single pass configuration (dashed line), irrespective of laser power.

Eq. (2) generalizes to

$$\frac{P_i^{(cav)}}{P_i} = \frac{1 - R_i - L_i}{(1 - \sqrt{R_i' C_i})^2}, \quad (4)$$

with L_i the loss on the input coupler and R_i' the total passive loss per cavity round trip. The resulting equations are solved numerically.³ The calculated conversion efficiency is shown in Fig. 2b as a function of the input coupler reflectivities, where a locus of points with maximal efficiency can be identified. Among them, a sensible choice is to select R_1 and R_2 close to each other to minimize the total intra-cavity power and thermal effects in the crystal. Note also that the optimum is quite loose, and that the reflectivities are relatively low, making the input coupler tolerant to small imperfections.

The generalized model including passive losses compares favorably to our experimental findings. Both the calculated steady state values (dashed lines in Fig. 1(b-d)) and the variation of output power P_3 with pump power P_1 (shown in Fig. 3a) are well-reproduced by the model. Furthermore, Fig. 3b shows no variation of the coefficient α defined in Eq. (1) even at the highest powers, thus validating the weakly

³The passive loss coefficients have been determined by injecting only one laser at a time in the cavity, and comparing the measured transmitted and reflected powers to the theoretically expected values.

depleted pump approximation. This also rules out additional effects (such as thermal effects related to absorption of the infrared beams) which would reduce α . Overall, we find that the model gives a reliable description of the SFG process for our experimental configuration, and allows one to optimize the parameters of the cavity to ensure maximum efficiency. A key parameter to achieve $\eta \simeq 0.9$ is the choice of a highly nonlinear crystal, resulting in a nonlinear loss $\alpha P_1^{(cav)}$ exceeding by far the roundtrip passive loss. With our set of parameters, we were able to reach output powers as high as $P_3 = 790$ mW or $\eta \approx 90\%$. This implies that our apparatus works very close to the theoretical ideal limit studied in the first part of the paper.

In conclusion, we presented an efficient all-solid state laser source based on SFG at 589 nm with input and output powers in the watt-level range. The source acts as a wavelength converter for the weakest source with a conversion efficiency around 90%. Such a setup can be used to produce other wavelengths in the visible range, provided the existence of input lasers at the right wavelengths. This provides a cost-effective solution for atomic physics experiment, free from the drawbacks of dye lasers.

We thank Pierre Lemonde for discussions. This work was supported by ANR, IFRAF, DARPA, and EU (MIDAS network). LdS acknowledges financial support from IFRAF.

References

1. R. Mildren, M. Convery, H. Pask, J. Piper, and T. McKay, "Efficient, all-solid-state, raman laser in the yellow, orange and red," *Opt. Express* **12**, 785 (2004).
2. D. Georgiev, V. P. Gapontsev, A. G. Dronov, M. Y. Vyatkin, A. B. Rulkov, S. V. Popov, and J. R. Taylor, "Watts-level frequency doubling of a narrow line linearly polarized raman fiber laser to 589nm," *Opt. Express* **13**, 6772 (2006).
3. Y. Feng, S. Huang, A. Shirakawa, and K.-I. Ueda, "589 nm light source based on raman fiber laser," *Jpn. J. Appl. Phys.* **43**, L722 (2004).
4. S. Sinha, C. Langrock, M. J. Dignonnet, M. M. Fejer, and R. L. Byer, "Efficient yellow-light generation by frequency doubling a narrow-linewidth 1150 nm ytterbium fiber oscillator," *Opt. Lett.* **31**, 347 (2006).
5. H. Moosmüller and J. D. Vance, "Sum-frequency generation of continuous-wave sodium d2 resonance radiation," *Opt. Lett.* **22**, 1135 (1997).
6. J. D. Vance, C. Y. She, and H. Moosmüller, "Continuous-wave, all-solid-state, single-frequency 400-mw source at 589 nm based on doubly resonant sum-frequency mixing in a monolithic lithium niobate resonator," *App. Opt.* **37**, 4891 (1998).
7. J. C. Bienfang, C. A. Denman, B. W. Grime, P. D. Hillman, G. T. Moore, and J. M. Telle, "20w of continuous-wave sodium d2 resonance radiation from sum-frequency generation with injection-locked lasers," *Opt. Lett.* **28**, 2219 (2003).
8. J. Janousek, S. Johansson, P. Tidemand-Lichtenberg, S. Wang, J. Mortensen, P. Buchhave, and F. Laurell, "Efficient all solid-state continuous-wave yellow-orange light source," *Opt. Express* **13**, 1125 (2005).
9. T. H. Jeys, A. A. Brailove, and A. Mooradian, "Sum frequency generation of sodium resonance radiation," *Appl. Opt.* **28**, 2588 (1989).
10. K. B. Davis, M. O. Mewes, M. R. Andrews, N. J. van Druten, D. S. Durfee, D. M. Kurn, and W. Ketterle, "Bose-einstein con-

- densation in a gas of sodium atoms,” *Phys. Rev. Lett.* **75**, 3969 (1995).
11. E. Streed, A. Chikkatur, T. Gustavson, M. Boyd, Y. Torii, D. Schneble, G. Campbell, D. Pritchard, , and W. Ketterle, “Large atom number bose-einstein condensate machines,” *Rev. Sci. Instrum.* **77**, 023106 (2006).
 12. R. W. Boyd, *Nonlinear optics* (Academic Press, 2003).
 13. G. D. Boyd and D. A. Kleinman, “Parametric interaction of focused gaussian light beams,” *J. Appl. Phys.* **39**, 3597–3639 (1968).
 14. J.-J. Zondy, D. Touahri, and O. Acef, “Absolute value of the d₃₆ nonlinear coefficient of aggas2: prospect for a low-threshold doubly resonant oscillator-based 3:1 frequency divider,” *J. Opt. Soc. Am. B* **14**, 2481 (1997).
 15. A. E. Siegman, *Lasers* (University Science Books, 1986).
 16. Y. Kaneda and S. Kubota, “Theoretical treatment, simulation, and experiments of doubly resonant sum-frequency mixing in an external resonator,” *Appl. Opt.* **36**, 7766–7775 (1997).
 17. E. Mimoun *et al.*, in preparation (2008).